

Scenario Discovery via Rule Extraction

Vadim Arzamasov

Karlsruhe Institute of Technology
Karlsruhe, Germany
vadim.arzamasov@kit.edu

Klemens Böhm

Karlsruhe Institute of Technology
Karlsruhe, Germany
klemens.boehm@kit.edu

ABSTRACT

Scenario discovery is the process of finding areas of interest, commonly referred to as scenarios, in data spaces resulting from simulations. For instance, one might search for conditions – which are inputs of the simulation model – where the system under investigation is unstable. A commonly used algorithm for scenario discovery is PRIM. It yields scenarios in the form of hyper-rectangles which are human-comprehensible. When the simulation model has many inputs, and the simulations are computationally expensive, PRIM may not produce good results, given the affordable volume of data. So we propose a new procedure for scenario discovery – we train an intermediate statistical model which generalizes fast, and use it to label (a lot of) data for PRIM. We provide the statistical intuition behind our idea. Our experimental study shows that this method is much better than PRIM itself. Specifically, our method reduces the number of simulations runs necessary by 75% on average.

KEYWORDS

scenario discovery, rule extraction, PRIM

1 INTRODUCTION

The behavior of many systems such as electrical grids or climate systems can be described with differential or difference equations. The resulting model connects a set of input values to the output and can be solved with computer experiments, aka. simulations. Analyzing data resulting from simulations has been of interest to the knowledge discovery community for a long time. Specifically, after performing simulation runs for different combinations of input values, it is often worth to replace the simulation model with a statistical or machine learning model, a so called *metamodel*, sometimes referred to as surrogate model, response surface model, replacement model [15] or model emulator [49]. Several authors give different reasons for doing so, including

- optimization of the simulated system [15, 27, 44, 52],
- design space exploration [15, 44, 52],
- sensitivity analysis [15, 27],
- model approximation [52],
- understanding relationships [44],
- risk analysis [27].

Although the items of this list are not clearly separated and can overlap, one can distinguish between the goals of high accuracy (optimization) and of having metamodels understandable for humans (design space exploration, risk analysis). One example task of the latter group has recently become known under the name *scenario discovery*, as we describe next.

The inputs of a simulation model can be classified into the ones which the user of the model (scientist, engineer, policy maker) can set, so-called *control* variables, and the ones reflecting uncertainty

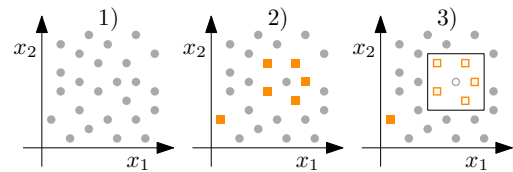


Figure 1: Scenario discovery process.

regarding specific conditions in which the modeled phenomena can take place, so-called *environmental* variables [41]. In the decision making literature, a set of values of the control variables is referred to as alternative [21], policy, or candidate strategy [7]; and the set of values of environmental variables is known as state of the world [7, 21] or alternative future [7]. The term *scenario* has several definitions in this context. In the narrowest sense, it refers to any single possible state of the world [21, 48]. Sometimes scenario refers to a set of states of the world where the policy fails to meet its goals [7, 10]. According to an even broader definition, a scenario is the regions of particular interest in the space of environmental inputs [25, 28, 29], for instance, where the output variable is above or below some threshold or takes a certain value. We use this last definition in this paper. Consequently, *scenario discovery* is the process of finding these interesting regions.

There are various degrees of uncertainty that one can associate with environmental variables [51], see also [49] for different sources of uncertainties. So-called *deep uncertainty* occurs when their distributions are not known, or the users of a simulation model do not agree on these distributions [7, 21]. In this case, one typically performs scenario discovery by

- (1) running several simulations for different combinations of environmental inputs drawn from a uniform distribution;
- (2) labeling the outcomes of interest with 1, the rest with 0;
- (3) applying a machine learning algorithm to find scenarios.

The algorithm used in the last step is usually PRIM [7]. It finds regions in the form of hyperboxes, one at a time [14]. See Figure 1. With PRIM, one typically evaluates the quality of the scenario with precision and recall metrics, referred to as density and coverage in the literature on scenario discovery; see for instance [7]. Another common metric is interpretability – a hyperbox restricting more dimensions of the space is less interpretable. Since a scenario targets at describing the internals of a ‘black-box’ simulation system rather than a particular data set resulting from several simulations, we propose a fourth quality metric – *consistency*. It quantifies the stability of a scenario discovered from different data sets describing the same phenomenon. Since simulations are often computationally expensive [52], one wants to obtain a scenario of high quality with a minimal number of simulations. In this paper we address the problem of reducing the number of simulation runs to obtain

high-quality scenarios or, equivalently, increasing the quality of scenarios discovered from a limited number of simulations. As we will show, a small number of observations affects PRIM very much, resulting in scenarios which are random to a high extent. This is, PRIM has a *high variance* or, equivalently, low consistency. Low-variance machine learning (ML) models, like random forests, provide more stable output, but hide their internal logic, i.e. humans cannot easily interpret them. But once they resemble the simulation model well enough, they can inexpensively label more data, which later serves as input of the scenario discovery method. Combining PRIM with a low-variance ML model is the main innovation of this paper.

Put differently, we propose a new scenario discovery process, by introducing an intermediate step of estimating an accurate meta-model and using it to obtain a larger data set to learn an interpretable model. Learning an interpretable model describing a more ‘complex’ one is called *rule extraction* [47]. We then come up with an analysis leading to the expectation that the proposed procedure works better than conventional ones from a statistical point of view. We also compare our method to conventional scenario discovery approaches with extensive experiments, using data from simulations of the electrical grid as well as 32 explicitly defined functions used in the metamodeling literature.¹ As a result, applying our technique results in significantly improved scenario discovery.

Paper outline: Section 2 reviews related work. Section 3 describes state-of-the-art approaches used for scenario discovery so far. Section 4 introduces our approach. Section 5 justifies our approach from a statistical point of view. Sections 6 and 7 describe the quality metrics used in the experiments and the experimental setup. Section 8 features the results. Section 9 concludes.

2 RELATED WORK

In this section we describe scenario discovery techniques used in the literature and justify our choice of PRIM. We then review improvements of scenario discovery with PRIM. Finally, we review work on rule extraction which has inspired our proposal.

Scenario Discovery Tools. PRIM is proposed for scenario discovery in [7, 10, 16–18, 21, 28–32] and many others, cf. [17]. Some authors [2, 18, 30, 32] use decision trees trained with the CART algorithm. Although not using the term *scenario discovery*, similar frameworks originated before: the authors of [39] use the GENREG algorithm, the ones of [55] use oblique rules, and the ones of [4] propose a fuzzy rule learning algorithm to analyze simulation outputs.

[32] compares CART and PRIM and concludes that the latter is more interactive and requires less post processing effort. CART has a high variance [5], meaning that the boxes vary highly for different data sets produced when simulating the same phenomenon, and it might include irrelevant attributes in the definition of the boxes [13]. This is undesirable according to [7, 28], but also holds for PRIM to some extent, as we will show.

All listed algorithms except for PRIM target at partitioning the input space into regions and assigning a class (interesting/uninteresting) to each of them. Accuracy is their main goal. Density and

coverage in turn are the primary target of PRIM and are most relevant in scenario discovery. In this paper we stick to PRIM, the state-of-the-art algorithm for scenario discovery.

PRIM Improvements. Several improvements of PRIM for scenario discovery were recently proposed. Normally, PRIM targets at maximizing the mean outcome value within a hyperbox; here, the function ‘mean’ is called peeling criterion. [29] studies alternative peeling criteria other than simple mean, also proposed in [14], and concludes that these alternatives are beneficial with heterogeneous inputs. [28] proposes using a bagging procedure. In fact, the authors use *bumping* [20], also proposed in [14], combined with random feature selection to increase the quality of PRIM. [10] combines PRIM with principal component analysis to produce oblique rules (PCA-PRIM). [7] complements PRIM with a ‘quasi p-value’ test to exclude insignificant attributes from the definition of the box.

We will compare our method to PRIM with bagging [28] and original PRIM. PCA-PRIM [10] and different peeling criteria [29] are orthogonal to this study.

Rule Extraction. Huysmans et al. [22] define the task of rule extraction as follows, “Given an opaque predictive model and the data on which it was trained, produce a description of the predictive model’s hypothesis that is understandable yet closely approximates the predictive model’s behavior”. A big variety of methods has been developed over the past decades. For instance, TREPAN [9], one of the most known methods, builds *m-of-n* decision trees (DT) using an opaque model, an artificial neural network (ANN) originally, as an oracle. The resulting tree was found to be more accurate than DT learned directly from the data used for ANN training, on four data sets. The CMM algorithm [11] works similarly, with C4.5 rules instead of DT and an ensemble of C4.5 rules instead of ANN.

Rule extraction can be treated as a subdomain of a larger area – model parroting (Section 7.5 in [43]). A representative method from this area is model compression [8]. The target is to replace a large model, an ensemble, which is expensive to store and execute but generalizes well, with a much ‘lighter’ and faster model, an ANN, which needs a big labeled dataset to avoid overfitting. The ensemble labels new training data for the ANN. The resulting ANN was more accurate than the one learned from the initial small data set.

The ideas used above are similar to our idea. However, the distinction lies in the final model to be trained. In the research mentioned, the final model is a ‘universal’ learner, a model which approximates any function with arbitrary accuracy given enough data. Thus, it is natural that the performance of the final model eventually converges to the one of the ‘intermediate’ model. With scenario discovery, the final model is a hyperbox, and accuracy is no longer the target – density and coverage are of interest.

3 SCENARIO DISCOVERY WITH PRIM

This section summarizes PRIM, followed by PRIM with bumping.

3.1 PRIM

The PRIM algorithm (Patient Rule Induction Method) was originally proposed in [14]; [20] (pp. 317–320) contains a concise description.

Let d, d_{val} be the datasets resulting from simulations; they contain D attributes $\{x_1, \dots, x_D\} = x$ corresponding to inputs of the

¹We share the code required to reproduce our experiments and figures: <https://github.com/Arzik1987/SDRE>

Algorithm 1: PRIM.peel (peeling step)

Data: $d, d_{val}, \alpha, box_0, minpts$ – as described in the text.
Result: sequence of nested hyperboxes

```
1  $j = 0$ ;  
2 while  $|d_{val}| > minpts$  &  $|d| > minpts$  &  $j < 99$  do  
3    $m = -1$ ;  
4    $j = j + 1$ ;  
5   for  $1 \leq i \leq D$  do  
6      $d^+ = d : d.x_i > l^+, |d^+| = (1 - \alpha) \cdot |d|$ ;  
7      $d^- = d : d.x_i < l^-, |d^-| = (1 - \alpha) \cdot |d|$ ;  
8     if  $avg(d^+.y) > m$  then  
9        $m = avg(d^+.y)$ ;  
10       $d = d^+$ ;  
11     if  $avg(d^-.y) > m$  then  
12        $m = avg(d^-.y)$ ;  
13       $d = d^-$ ;  
14    $box_j = adjust(box_{j-1}, d)$ ;  
15    $d_{val} = d_{val} : d_{val}.x \in box_j$ ;  
16    $m_{val}(j) = avg(d_{val}.y)$ ;  
17  $r = arg\ max_j (m_{val}(j))$ ;  
18 return  $\{box_0, \dots, box_r\}$ 
```

simulated model, and variable y , the output. We assume that $y = 1$ for the cases of interest and $y = 0$ otherwise. The number of rows N in d is the number of simulation runs. We refer to the values $\{x_i^k, \dots, x_D^k\}$ in the k -th row of d or d_{val} as *point*.

The algorithm works in two steps, called *peeling* and *pasting*. We describe them separately. Algorithm 1 is the peeling step. It starts with the whole dataset d and the D -dimensional box box_0 containing it. Then it repeatedly ‘peels out’ α points from the data with a hyperplane orthogonal to one dimension, so that the mean value of y of the remaining points is maximal (Lines 5–13), and it adjusts the box so that it is a minimal bounding rectangle of these remaining points (Line 14). Here α is the *peeling parameter* [14] and denotes the *share* of points. This is done until the stopping criterion is met. In our case, it is the minimum number of points $minpts$ of the train set d or validation set d_{val} contained in the box, or the number of iterations of the while loop. We restrict the latter to 99 (Line 2). Finally, the hyperbox with the highest mean on d_{val} (Line 17) is returned together with all preceding boxes (Line 18). The rationale is to let a domain expert choose the one which best suits their needs. Pasting works similarly but in the opposite direction. It expands one of the hyperboxes obtained after the peeling step as long as the mean of y of the points contained in it does not decrease. Section A.1² describes this in detail.

Many studies [10, 28, 29] compare PRIM modifications considering only the peeling phase. We also confine ourselves to the peeling algorithm but show experimentally that this simplification does not influence the results significantly. PRIM with bumping and our method include only the peeling step.

²Hereafter sections containing letter in their names refer to Appendix.

Algorithm 2: PRIM with rule extraction

Data: $d, d_{val}, \alpha, box_0, minpts, K, AM$ – described in the text
Result: sequence of nested hyperboxes

```
1  $f^a = train(AM, d)$ ;  
2  $d_{new}.x = new.points(K)$ ;  
3  $d_{new}.y = predict(f^a, d_{new})$ ;  
4  $boxes = PRIM.peel(d = d_{new}, \dots)$ ;  
5 return  $boxes$ 
```

3.2 PRIM with Bumping

The PRIM algorithm with bumping [28] produces multiple boxes by varying the dataset d and returns only the ones not dominated by any other box in terms of coverage and density. We define density, coverage, and other quality measures in Section 6.

Definition 3.1. For a set of quality measures $\{Q_1, \dots, Q_n\}$, a box with the values $\{q_1^i, \dots, q_n^i\}$ of these measures is dominated by a box with values $\{q_1^j, \dots, q_n^j\}$ if $\forall r \in \{1, \dots, n\} : q_r^j \geq q_r^i$.

The PRIM algorithm with bumping works as follows.

- (1) Take a random bootstrap sample d_{bs} from d ;
- (2) take a random subset S of t attributes from d ;
- (3) run Algorithm 1 with $d = d_{bs}$ using only attributes S ;
- (4) repeat Steps (1)–(3) T times;
- (5) return the hyperboxes not dominated in terms of the density-coverage metrics on the validation set d_{val} .

We observe that the word ‘bagging’ proposed in [28] as the name of this method is misleading. Since no averaging over several models takes place, the original term *bumping* is correct [14, 20]. See Section A.2 for a formalization.

4 PROPOSED METHOD

The novelty of our approach is the introduction of an intermediate step to train a metamodel with low variance and generalization error (Algorithm 2). The new process consists of the following steps.

- (1) Using the dataset d , train an accurate metamodel AM ;
- (2) uniformly sample K new points from the area described by the hyperbox box_0 containing all points of d ;
- (3) label these points using the trained metamodel f^a to form a new dataset d_{new} ;
- (4) run Algorithm 1 with d_{new} instead of d .

In the rest of the paper, we use random forest [6] as the intermediate metamodel. The rationale is that random forests were shown to perform well in various classification tasks [50].

5 PRIM ON SMALL DATASETS

In this section we demonstrate why original PRIM has difficulties in learning scenarios of high quality from small data sets, and how our method overcomes them. We do so both from a statistical point of view and with an example.

5.1 Statistical Intuition

Bias-Variance Decomposition. Let f denote the function described by the simulation model. In each iteration j of the peeling stage,

PRIM compresses the box_{j-1} to obtain the box box_j . It chooses box_j from candidate boxes – we name them box_{ij} , $i = 1, \dots, 2D$ – so that the mean value of f in it is maximal. Equivalently, the mean value of f in the box $b_{ij} = box_j \setminus box_{ij}$ which is ‘peeled out’ is minimal. In reality, f is unknown, and its mean μ_{ij} in b_{ij} is estimated from the sample of points contained in b_{ij} . A high error of this estimate may result in cutting off the wrong box, i.e., the one which does not maximize the mean value of f in box_j . That is, our method will make fewer wrong cuts if its error in estimating μ_{ij} is smaller than with the original method.

Let us pick some $b \in \{b_{ij}\}$. The mean value of f in b is

$$\mu = \frac{\int_b f(x)p(x) dx}{\int_b p(x) dx}. \quad (1)$$

Here $p(x)$ stands for the pdf of the D -dimensional random variable X denoting the point in the input space. In the following analysis, we assume b to be fixed. It contains $n = \alpha \cdot (1 - \alpha)^d \cdot N$ points labeled with $y_r = f(x^r)$, $r = 1, \dots, n$ by means of simulations. The estimate of mean μ from the data then is

$$\hat{\mu} = \frac{1}{n} \sum_{r=1}^n y_r \quad (2)$$

The mean squared error (MSE) [14] of this quantity is

$$MSE_O = \mathbb{E}[\mu - \hat{\mu}]^2 = (\mu - \mathbb{E}\hat{\mu})^2 + \mathbb{E}[\hat{\mu} - \mathbb{E}\hat{\mu}]^2 = [\text{Bias}(\hat{\mu})]^2 + \text{Var}(\hat{\mu}) \quad (3)$$

Here the expectation is taken over all datasets d with $|d| = N$ containing points i.i.d. from $p(x)$. Under deep uncertainty, one accepts the uniform distribution of model inputs, i.e., $p(x) = \text{const}$, and samples x^r i.i.d. from it. Assuming that there is no noise induced by the simulation process, $\hat{\mu}$ is an unbiased estimate of μ . Remember that y_r takes values from $\{0, 1\}$. Thus, y_r is a Bernoulli random variable with $\Pr(y_r = 1) = \mu$. Written formally,

$$\text{Bias}(\hat{\mu}) = 0, \quad \text{Var}(\hat{\mu}) = \frac{\mu(1 - \mu)}{n} = MSE_O \quad (4)$$

With our method, a function f^a learned with metamodel AM is used to label points. Let μ^a be the mean value of f^a within b and

$$\hat{\mu}^a = \frac{1}{k} \sum_{r=1}^k y_r^a \quad (5)$$

be its estimate where $y_r^a = f^a(x^r)$, and $k \approx n \cdot K/N$ is the number of new points inside b ; see Section 4 for an explanation of K .

Assume first that $y_r^a \in \{0, 1\}$. Then $\Pr(y_r^a = 1) = \mu^a$. In general, $\mu^a \neq \mu$. For a fixed function f^a , analogously to (3)–(4), the bias-variance decomposition of the mean squared error is

$$\begin{aligned} [\text{Bias}(\hat{\mu}^a)]^2 &= (\mu - \mu^a)^2, \\ \text{Var}(\hat{\mu}^a) &= \frac{\mu^a(1 - \mu^a)}{k} \xrightarrow{k \rightarrow \infty} 0 \end{aligned} \quad (6)$$

where the expectation was taken over all datasets d_{new} (Algorithm 2, Line 2) that are possible with our approach. The MSE with our method using metamodel AM for large K is

$$MSE_{AM} = \mathbb{E}[\mu - \mu^a]^2 \quad (7)$$

where the expectation is taken over all feasible datasets d as in (3), and all possible fits f^a of a given metamodel AM obtained on them.

Now we can compare the MSE_O obtained with the original approach (4) with MSE_{AM} with our approach (7). Assuming that the best scenario is the one discovered with PRIM knowing the true function f , our method will perform superior if for all possible boxes b , $\mathbb{E}[\mu - \mu^a]^2 < \mu(1 - \mu)/n$. Similarly, our method is *likely* to show better performance than original PRIM if the above inequality holds for the *majority* of boxes. Note that the left-hand side of the inequality implicitly depends on N , as increasing the number of training examples typically leads to a higher accuracy of f^a and to a lower value of $\mathbb{E}[\mu^a - \mu]^2$. Now consider the model AM which outputs class probability estimates instead of classes, i.e., $y_r^a \in [0, 1]$. Interestingly, in this case, our approach may outperform the original one even when the size K of the new data set d_{new} is comparable to the size N of the initial dataset d . Specifically, the following holds.

PROPOSITION 5.1. *If $n = k$ and $\mu = \mu^a$, then $\text{Var}(\hat{\mu}^a) \leq \text{Var}(\hat{\mu})$*

PROOF. Since $n = k$, it is sufficient to show that

$$\mathbb{E}[y_r^a]^2 - (\mathbb{E}y_r^a)^2 = \text{Var}(y_r^a) \leq \text{Var}(y_r) = \mu(1 - \mu) \quad (8)$$

Since $\mathbb{E}y_r^a = \mu$, (8) $\iff \mathbb{E}[y_r^a]^2 \leq \mu$. This is true as

$$\mathbb{E}[y_r^a]^2 = \int_0^1 (y_r^a)^2 g(y_r^a) dy_r^a \leq \int_0^1 y_r^a g(y_r^a) dy_r^a = \mu.$$

Here $g(y_r^a)$ is the pdf of y_r^a implied by the restriction of f^a to the box b . The latter inequality holds since $y_r^a \in [0, 1]$ and $g(y_r^a) \geq 0$. \square

However, the condition $\mu = \mu^a$ of the above proposition does not hold for all possible boxes b , unless $f \equiv f^a$. We experiment with the performance of our approach in case $K = N$ in Section 8.2.2.

Finally, when the simulation process is imperfect and introduces noise, in general $\Pr(y_r = 1) \neq \mu$. Consequently, $\text{Bias}(\hat{\mu})$ in (4) is no longer zero, and the analysis becomes more sophisticated. We evaluate the influence of noise experimentally (Section 8.2.3).

Discussion of the Statistical Derivations. To avoid restrictive assumptions on the true function f , we made certain simplifications for the analysis. First, we assumed that the box b and the number of points it contains, n , are fixed simultaneously, while the points in d are sampled at random. In reality, only n is fixed at each iteration, and the box boundary varies to include exactly n points (Algorithm 1, Lines 6–7). Allowing the box boundary to vary with different realizations of d would make MSE estimates (4) and (6) incomparable. Second, one usually uses so-called space filling designs to form a dataset d rather than ‘brute force’ random sampling, e.g., Latin hypercube sampling [27]. Generally, this would result in lower variance values, than values estimated with (4) or (6). Despite these simplifications, we believe that our analysis provides convincing explanations of the results obtained in this paper.

5.2 Example

We now check the validity of our analysis and provide a synthetic example where our method yields much better output than the original one. To this end, we use data generation process (DGP) #3 from [10]. Here the label y only depends on two inputs, x_1 and x_2 , as $y = 1$ if $x_1 > 0.6$ and $x_2 > 0.8$. Finally, DGP3 adds some noise by inverting 0.2% of the labels. The support of DGP3 is $x_i \in [0, 1]$, $i = 1, \dots, 5$.

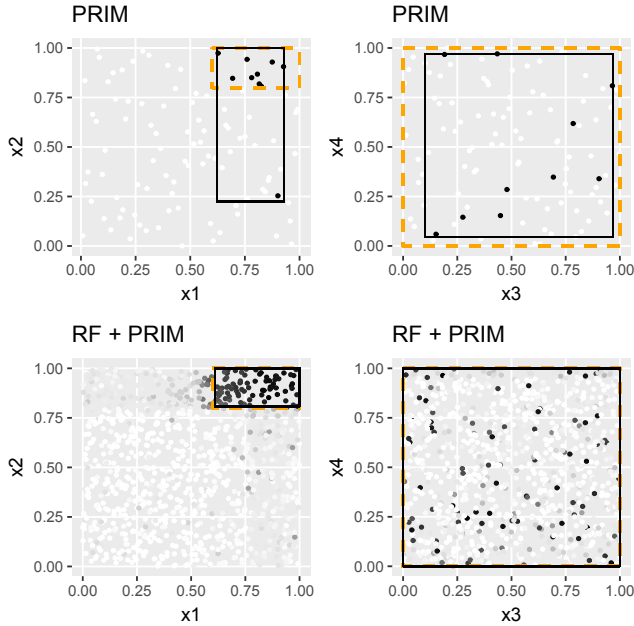


Figure 2: The results obtained with original PRIM and with our proposed method on the example dataset.

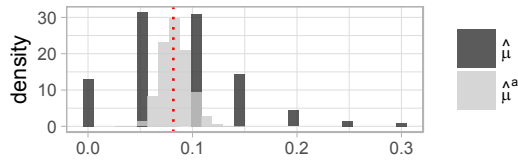


Figure 3: The distributions of $\hat{\mu}$ (dark) and $\hat{\mu}^a$ (light)

Mean-Squared Error. We use random forest, which outputs probabilities, as metamodel. We set $N = 400$ and estimate the MSE of the μ estimate for box b defined as $x_3 > 0.95$ ($\alpha = 0.05$). The expected number of points in this box is $n = \alpha \cdot N = 20$, and $\mu \approx (1 - 0.6)(1 - 0.8) = 0.08$. We neglected the noise in the last calculation. The variance of the original method, calculated using (4), is $\sigma = 0.08 \cdot (1 - 0.08)/20 = 3.68 \cdot 10^{-3}$. MSE_O obtained in experiments is $3.54 \cdot 10^{-3} \approx \sigma$, whereas MSE_{AM} are $2.9 \cdot 10^{-3}$ and $0.19 \cdot 10^{-3}$ for $K = 400$ and $K = 10^5$ respectively. That is, $MSE_O > MSE_{AM}$. This result holds for eight (for $K = 400$) and nine (for $K = 10^5$) boxes out of ten candidates for cutting off at the first iteration of the peeling step of PRIM. Figure 3 illustrates the experiment. It shows distributions of $\hat{\mu}$ and $\hat{\mu}^a$ ($K = 10^5$) for b ; the dotted line is the true μ . See Section B for more details and further discussion.

Comparing Scenarios. For this study, we set $N = 100$. Figure 2 graphs the result obtained with original PRIM and with our method (solid thin lines). Four dimensions $\{x_1, \dots, x_4\}$ are presented. Dashed thick lines represent the true scenario.

The top two plots show the 100 points obtained directly from DGP3. White points stand for $y = 0$ and black ones for $y = 1$. The

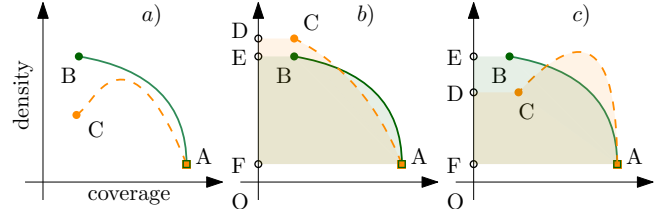


Figure 4: Mutual positions of two peeling trajectories

plots reveal that PRIM makes mistakes by cutting the box in the irrelevant space $\{x_3, x_4\}$. It does so for the following reasons:

- There are nine true scenario examples ($y = 1$) – not enough to fill the range of irrelevant attributes $\{x_3, x_4\}$. So there are some areas near axes in these coordinates with no scenario examples, for instance near the axis x_4 .
- One point, near the bottom of the left upper plot, is wrongly labeled with $y = 1$ (noisy data). It prevents the algorithm from further restricting the box in this space before all cuts in other dimensions leading to better results are made.
- The algorithm stops when the learned box contains $minpts = 20$ points. Since there are only nine true scenario examples, this box contains at least 11 irrelevant ones. In other words, the box is too big to properly describe the scenario but cannot be further reduced due to a lack of points in d .

The bottom two plots graph the 1000 newly generated points labeled with random forest. The color of points stands for their probability of belonging to scenario $y = 1$, changing from white ($\Pr(y = 1) = 0$) to black ($\Pr(y = 1) = 1$). Clearly, this new data set allows PRIM to learn a better scenario by overcoming the issues of the original data set just described.

6 PRELIMINARIES: QUALITY METRICS

In this section, we describe the quality metrics we use to compare the different algorithms. We assume that, to estimate these metrics, one uses a separate data set of points d_{test} labeled by the simulation model which does not overlap with d and d_{val} .

6.1 Coverage, Density, Interpretability

Assume that d_{test} contains N_1 examples with $y = 1$ and N_0 examples with $y = 0$. For the learned hyperbox describing the scenario, the corresponding numbers are S_1 and S_0 . A natural target is that the scenario contains as many points of interest $y = 1$ and as few uninteresting examples with $y = 0$ as possible. Coverage and density quantify the degree to which these goals are achieved [7].

$$coverage = \frac{S_1}{N_1} \quad density = \frac{S_1}{S_1 + S_0}$$

These quantities correspond to recall and precision used in the statistical learning literature [26].

As described before, PRIM does not produce a single box; instead, it outputs a sequence of boxes from which a user can choose one. This choice is typically made by compromising between density and coverage [7]. To exclude this subjective choice from our evaluation, we compute the metrics for each box in the sequence. Each such sequence forms a curve on the density-coverage plain, a.k.a. *peeling*

trajectory [7, 14]. To rank two algorithms, we compare their curves: AB and AC on Figure 4. If the boxes of one algorithm dominate the boxes of the other one, like in Plot a), the conclusion is straightforward: The algorithm which has yielded AB is better. When the peeling trajectories intercept each other, the area under the curve (AUC) quantifies the quality. This is, we compare the areas covered by figures $ABEF$ and $ACDF$ as shown in Plots b) and c).

Sometimes one wants to find scenarios as pure as possible, i.e. to maximize the density while allowing lower coverage. Since the test data is not available in reality, this choice can be made using validation data. In our case, this corresponds to choosing the last box returned by Algorithm 1. Thus, we will also compare the densities of the last boxes produced by different methods.

Interpretability is another quality metric often used in scenario discovery. A hyperbox already is quite an interpretable model output [13, 23]. However, one can additionally compare scenarios by the number of dimensions restricted by the hyperboxes defining them [7, 28]. As with density, we will do such a comparison with the last boxes returned by each algorithm.

6.2 Consistency

Some models used for scenario discovery, e.g., decision trees, are known to have *high variance* [26]. This means that, for the same DGP, the resulting model very much depends on the exact data set used to train it. This is an undesired property of a scenario discovery method. It reduces interpretability [14] since one looks for some hidden structure in DGP rather than in the particular data produced by it. Thus, we introduce the fourth quality measure for scenarios – *consistency* – the extent of robustness of the learned scenario against the changes in the data set.

Definition 6.1. For two datasets d_1 and d_2 , $|d_1| = |d_2|$ produced with the same DGP, let box_1 and box_2 be the scenario descriptions obtained with the same algorithm A . Let V_o be the volume of the overlap of these boxes and V_u the one of the union of box_1 and box_2 . The consistency of A is

$$consistency = V_o/V_u$$

In contrast to the measures density, coverage and interpretability, consistency is not applicable to a single box output by the algorithm, but compares the boxes computed on two data sets.

Consistency is often used in the rule learning literature. However, it has different definitions. For instance, [22] defines it as the inherent randomness of the algorithm, not the one resulting from the choice of the training data.

7 DATA AND EXPERIMENTAL SETUP

For our experimental study we use 32 DGPs defined by explicit functions and one simulation model – the decentral smart grid control (DSGC). Below we shortly describe these data sources as well as the methodology of the experiments.

7.1 DGPs Defined with Explicit Functions

We have used different sources of DGPs. First, we have implemented DGPs 1–8, and 101, and 102 from [10] using the descriptions in the appendix of that paper. All these DGPs are ‘noisy’ with probability 0.2% of having the false label. For DGPs 1, 3, 5–7, we obtained data

Table 1: Experimental setting

	B	B.all	O	O.p	RF (l or p)
α	0.05				
$ d $	{400, 800, 1600} +{200, 1200, 2000} – for DSGC				
$minpts$	20				
β	×	×	×	0.01	×
t	$\lceil\sqrt{D}\rceil$	D	×	×	×
T	50		×	×	×
K	×	×	×	×	100000

similar to that presented in Figure 2 in [10], but for DGPs 2, 4 and 8 the plots were different. With DGP 101, we did not get any examples labeled with $y = 1$ and thus excluded it from our analysis. The DGPs ‘morris’ and ‘sobol’ are the functions implemented in the R package ‘sensitivity’³. The DGP ‘ellipse’ is constructed by us as described in Section C. Finally, we used the R implementations of the other DGPs from [46]. These functions are used to test input variable screening and sensitivity analysis in simulations. We keep the original names of the functions as provided by the implementation. We converted continuous function output to binary by specifying the threshold thr , so that $y = 1$ if the output is below thr and $y = 0$ otherwise; this is common in scenario discovery [7]. For more detailed information and references, see Section C.

7.2 Use Case – DSGC Simulation

Decentral smart grid control (DSGC) [42] is a novel approach realizing demand response without a centralized IT infrastructure. The key idea is to connect the electricity price to the local frequency of the electricity grid at each consumer or supplier. Specifically, each participant measures the frequency at its location, averages this frequency over time and reacts by adapting its electricity consumption or production with a delay. Simulations of this system allow to study its stability for different input values. In the following, we will work with a toy example consisting of five actors – four consumers and one producer. For more information, see Section D.

7.3 Experimental Setup

Here we discuss the choice of hyper-parameters for the algorithms and how we perform our experiments.

7.3.1 Hyper-parameters. The three algorithms described above – original PRIM, PRIM with bumping and our approach, – have certain hyper-parameters in common. We set the peeling parameter $\alpha = 0.05$, as it is the most typical choice in the literature. Next, we set the stopping criterion $minpts = 20$. For all DGPs, we experimented with data sets of three sizes: $|d| = \{400, 800, 1600\}$. For DSGC the sizes are $|d| = \{200, 400, 800, 1200, 1600, 2000\}$. We consider two versions of original PRIM: without pasting – ‘O’, and with the pasting step – ‘O.p’. With ‘O.p’, pasting is with pasting parameter $\beta = 0.01$ for each box in the sequence resulting from ‘O’. The hyper-parameter values for PRIM with bumping were not stated in the respective paper [28]. We set the number of iterations

³<https://cran.r-project.org/web/packages/sensitivity/index.html>

Table 2: AUC across different DGPs

$ d $		B	B.all	O	O.p	RF.l	RF.p
400	avg	42.8	42.4	41.3	41.2	48.7	49.1
	# 1	1	0	0	0	8	24
	# 2	0	1	0	0	24	8
800	avg	46.4	46.7	46.4	46.3	50	50.5
	# 1	0	1	0	0	5	27
	# 2	4	0	0	0	24	5
1600	avg	48.3	49.3	49.1	49	50.8	51.2
	# 1	0	1	0	0	5	27
	# 2	6	0	0	0	22	5

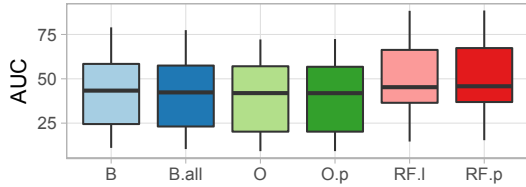


Figure 5: AUC across different DGPs for $|d| = 400$

$T = 50$. We consider two variants of this algorithm which differ in the number of attributes t used in each iteration. ‘B’ uses $t = \lceil \sqrt{D} \rceil$ attributes, the common value used in random forest for classification, where D is defined in Section 3.1; ‘B.all’ uses all attributes – $t = D$. Finally, we set the number of new points generated and labeled with our approach to $K = 10^5$, i.e. much larger than any $|d|$ used. As mentioned, we use random forest as the ‘complex’ metamodel in Algorithm 2. To set its hyper-parameters, we use the default hyper-parameter optimization procedure of package ‘caret’⁴. Random forest can return either class labels (0 or 1) or class probabilities for the new K points yielding two variants of our algorithm, ‘RF.l’ and ‘RF.p’. Table 1 summarizes the above.

7.3.2 Design of Experiments. To form the datasets $d = d_{val}$, we use Latin hypercube sampling for DGPs defined with explicit functions and Halton sequence [19] for DSGC simulations. For each DGP, we independently generated the test data d_{test} containing 10^4 points. We repeat the experiment 50 times for each DGP and each value of $|d|$. We compute consistency for each pair of the last boxes from different runs and then average the results; this is in line with the approach in [11] to compute stability – a measure similar to consistency.

8 RESULTS

We first compare the performance of approaches across all DGPs. We then present the results of further experiments with DSGC where we study how the values of $|d|$, K and noise influence the performance of the methods. More detailed results are in Section E.

8.1 Performance across All DGPs

We present the results for the four metrics in a form which we now explain, taking AUC as an example. First, for each DGP and each

⁴<http://topepo.github.io/caret/index.html>

Table 3: Density across different DGPs

$ d $		B	B.all	O	O.p	RF.l	RF.p
400	avg	80.9	81.7	81.1	80.9	91.4	92.6
	# 1	1	0	0	0	2	30
	# 2	2	1	0	0	28	2
800	avg	86.3	87.1	87	86.9	93.9	95.2
	# 1	0	1	0	0	1	31
	# 2	6	0	0	0	26	1
1600	avg	89.8	91.2	91.1	90.9	95.2	96.6
	# 1	0	1	0	0	1	31
	# 2	10	0	0	0	22	1

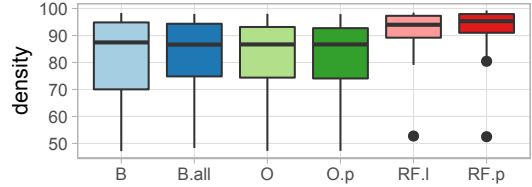


Figure 6: Density across different DGPs for $|d| = 400$

Table 5: Number of irrelevant dimensions restricted

$ d $	B	B.all	O	O.p	RF.l	RF.p
400	0.38	2.78	2.78	2.78	0.1	0.37
800	0.29	2.67	2.35	2.36	0.12	0.49
1600	0.28	2.59	2.18	2.19	0.1	0.71

value of $N = |d|$ we averaged AUC values across 50 experiments. Figure 5 plots these averages; each box is based on the 33 DGPs under consideration. The average AUC values over 50 experiments and 33 DGPs for each dataset size, $|d|$, are in row ‘avg’ in Table 2. For a rather high number of points, $|d| = 1600$, the differences in these values between original PRIM and our methods are low. But for some DGPs our method still improves the results of original PRIM significantly (Section E). For each DGP we also recorded which methods performed best and second best. The counts of these numbers are in rows ‘#1’ and ‘#2’ in Table 2 respectively. These results show that in general our method (‘RF.l’ and ‘RF.p’) outperforms the existing ones in terms of AUC.

The results for density are presented in Figure 6 and Table 3. Again, our method performs well in most cases. The minimal density achieved by it is much higher than that of competing methods.

Figure 7 and Table 4 feature results regarding the number of restricted dimensions. Smaller numbers, standing for higher interpretability, are better. Note that the comparison with ‘B’ is not fair, since the number of attributes used in the box definition under ‘B’ is restricted ‘manually’ ($t = \lceil \sqrt{D} \rceil$) and usually does not fall together with the number of inputs actually influencing the simulation result. But even in this case, our method often performs better, demonstrating its ability to distinguish between influential and not significant inputs, even with moderate volumes of data.

More detailed results show that our method, ‘RF.l’, often approximates the number of inputs affecting the output better than any

Table 4: Number of restricted dimensions

$ d $		B	B.all	O	O.p	RF.I	RF.p
400	avg	3.3	7.72	7.71	7.71	3.63	4.24
	# 1	15	0	0	0	20	3
	# 2	9	0	0	0	13	7
800	avg	3.25	7.72	7.36	7.37	3.87	4.67
	# 1	15	0	0	0	19	1
	# 2	11	0	0	0	14	6
1600	avg	3.22	7.57	7.14	7.14	3.99	5.04
	# 1	17	0	0	0	17	1
	# 2	13	0	0	0	15	3

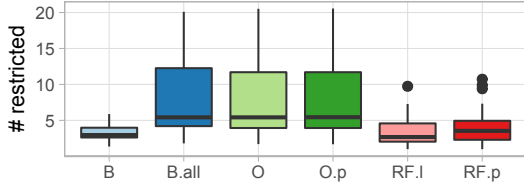


Figure 7: Interpretability across different DGPs for $|d| = 400$

Table 6: Consistency across different DGPs

$ d $		B	B.all	O	O.p	RF.I	RF.p
400	avg	42.3	41.5	42.6	43.3	53.3	51
	# 1	1	0	0	2	19	11
	# 2	3	0	3	2	10	15
800	avg	42	44.1	45.1	45.5	55.6	52.5
	# 1	0	1	0	1	19	12
	# 2	4	3	2	2	10	12
1600	avg	41.7	46.1	47.2	47.6	58.5	53.8
	# 1	1	2	0	1	19	10
	# 2	5	4	2	0	11	11

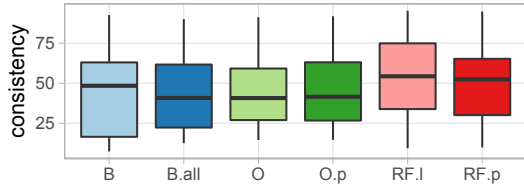


Figure 8: Consistency across different DGPs for $|d| = 400$

competitor. To see this, we first selected 19 DGPs where the maximal number of influencing dimensions I_j ($j = \{1, \dots, 19\}$) is lower than the total DGP dimensionality D_j (see Section E). For each such DGP, we calculated the difference between the average number of dimensions restricted by each method in 50 experiments and I_j . We then kept only positive values – meaning that irrelevant dimensions are restricted – and averaged the results. See Table 5. Clearly, ‘RF.I’ is the leader providing the fewest irrelevant restrictions.

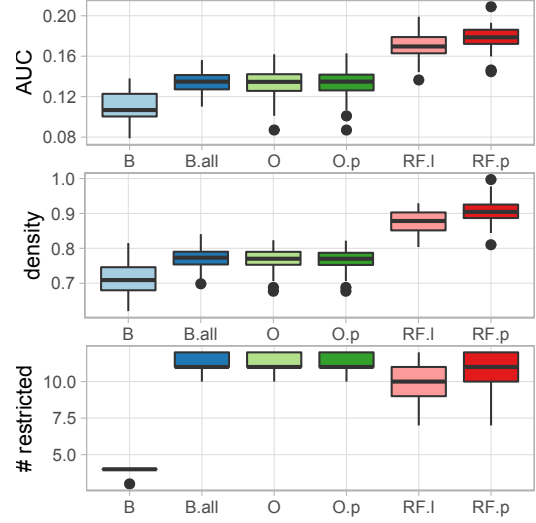


Figure 9: Quality metrics for DSGC for $|d| = 400$

Finally, Figure 8 and Table 6 contain results regarding consistency. Our approach, rule extraction, again is superior. The gap between it and competitors grows with the size of the data set $|d|$.

On average, the levels of AUC, density and consistency achieved for $|d| = 1600$ with conventional methods are comparable to those achieved with $|d| = 400$ with ‘RF.I’ and ‘RF.p’. In other words, our approach can reduce the number of simulation runs by $\approx 75\%$. All in all, we recommend to use ‘RF.I’ to obtain larger, more consistent and more interpretable scenario descriptions and to use ‘RF.p’ when high density is the top priority.

8.2 In-depth Experiments with DSGC

Figure 9 plots quality metrics for DSGC with $|d| = 400$ across different methods obtained in 50 experiments. One can see that our approach yields a significant improvement as measured with AUC or density over the alternatives. With regard to interpretability, method ‘B’ restricts the smallest number of dimensions, as this number is forced to be $t = \lceil \sqrt{D} \rceil = 4$. In case of DSGC, this restriction is too hard as more attributes do influence the simulation output. Thus, the actual benefit in interpretability with ‘B’ is arguable, while the other quality measures suffer. The outputs of the other five methods are similarly interpretable restricting 10–12 dimensions for the data set. This result does not vary much in subsequent experiments, and we skip respective comparisons in what follows.

Figure 10 plots the peeling trajectories for DSGC with $|d| = 400$ for different methods smoothed across 50 experiments. The curves produced by our approach dominate the ones obtained with competitors, i.e. lead to both higher density and coverage.

8.2.1 Different Values of $|d|$. Figure 11 shows the AUC, density and consistency values for DSGC simulations depending on the number of points in d averaged across 50 runs. The horizontal axis is logarithmically scaled. AUC and density values obtained using our approach are always greater than those of competing methods. For small d , consistency of our method is somewhat lower than that of the original PRIM and of PRIM with bumping. This is

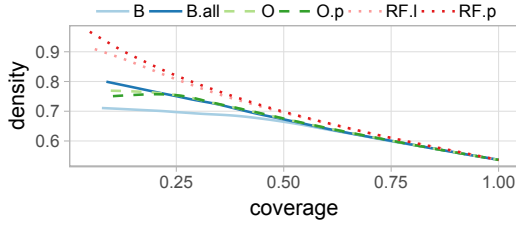


Figure 10: Peeling trajectories for DSGC for $|d| = 400$

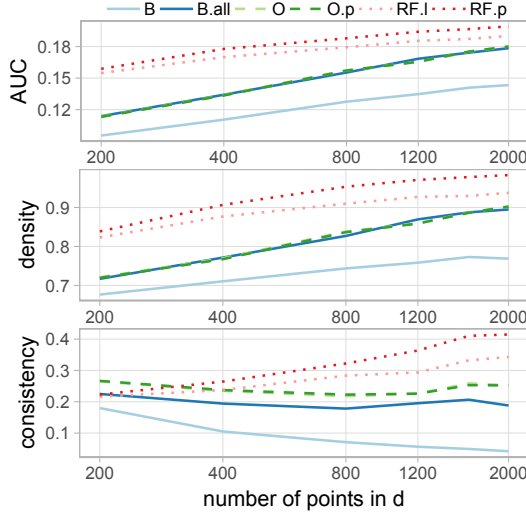


Figure 11: Quality metrics for DSGC in dependence on $|d|$

because the boxes produced by our method tend to be smaller. This results in smaller areas of overlap while allowing higher density. Note that generating boxes of very different size is not exactly fair when comparing consistency of the algorithms. Indeed, the most consistent algorithm is one doing nothing but returning the box containing all data. Such algorithm is clearly useless. However, with the growth in $|d|$, consistency of ‘RF.I’ and ‘RF.p’ grows, while consistency of the other approaches first declines to reach its bottom value. For $|d| > 800$, our approach is better.

8.2.2 Different Values of K . We investigate how the number of newly generated and labeled points K influences the performance of our methods. We started with $|d| = 400$ and experimented with different values of K . Note that our approach applies PRIM only to K newly generated and labeled points, ignoring the initial data resulting from simulations. Figure 12 graphs the results averaged across 50 runs. For both AUC and density, ‘RF.p’ (when random forest outputs probabilities) is better than ‘RF.I’ (when labels $\{0, 1\}$ are predicted) and stops improving at $K \approx 1600$. For ‘RF.I’ the density continues to improve even for $K > 25000$.

A very interesting outcome is that ‘RF.p’ outperforms the other methods even when $200 = K < |d| = 400$. That is, 200 points labeled with probabilities learned with random forest let PRIM induce a better scenario than 400 points labeled with $\{0, 1\}$ with the original simulation model. This result confirms our statistical analysis.

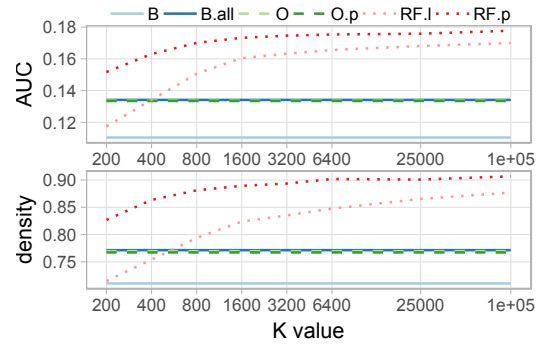


Figure 12: Quality metrics for DSGC in dependence on K for $|d| = 400$

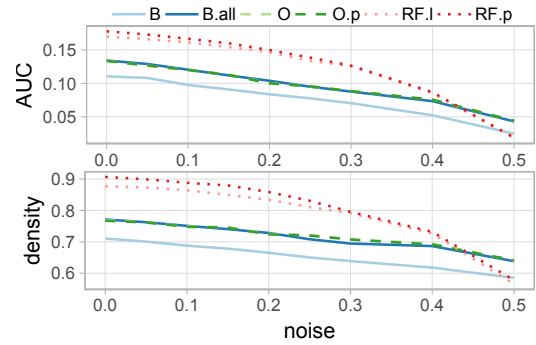


Figure 13: Quality metrics for DSGC in dependence on noise level for $|d| = 400$

8.2.3 Different Noise Levels. Finally, we experiment with different levels of noise in the data. We assume that the noise has the form of a random flip of the label value ($0 \rightarrow 1$ or $1 \rightarrow 0$), i.e., is independent of the model inputs $\{x_1, \dots, x_D\}$ and the true label y . The noise level then reflects the share of points chosen at random for which the label is changed. Noise level 0.5 implies completely random data with $\Pr(y = 1) = \Pr(y = 0) = 0.5$. Figure 13 contains the results for $|d| = 400$ averaged across 50 runs. As expected, scenario quality decreases with the level of noise. Our approach provides better results for any level we experimented with, except 0.5. For random data, when the noise level is 0.5, the AUC value is positive, and the density (0.57–0.64) is greater than that on the entire test set d_{test} (0.54). This is due to the best scenario being ‘inside’ the initial box and thus even cutting off any dimension at random results in the increased density at first.

9 CONCLUSIONS

Simulations let us study the behavior of complex systems. Scenario discovery, the topic of this paper, is the process of using simulations to gain interpretable insights regarding this behavior. PRIM is the state-of-the-art method for scenario discovery. It isolates conditions for system behavior of interest (e.g. system instability), in the form of a hyperbox, referred to as a scenario. The disadvantage of this method, as we have shown, is that it requires relatively large

numbers of simulation runs, particularly in high dimensions, i.e. for systems with many input variables. Since simulations are often computationally hard, this is prohibitive in many cases.

In this paper, we have studied reducing the number of simulations needed to discover good scenarios. Based on data produced with simulations, our method first trains a powerful, but complex statistical model. This model is then used to replace the simulation model, to label much more data for PRIM. We have justified the plausibility of our approach from a statistical point of view as well as with exhaustive experiments. The experiments show that our method is much better than conventional ones. More specifically, it requires 75% fewer points than a conventional one on average to produce scenarios of comparable quality.

ACKNOWLEDGMENTS

This work was supported by the German Research Foundation (Deutsche Forschungsgemeinschaft), Research Training Group 2153: “Energy Status Data – Informatics Methods for its Collection, Analysis and Exploitation”. We also thank Georg Steinbuss, Edouard Fouche for fruitful discussions and Tien Bach Nguyen for help with the code.

REFERENCES

- [1] Jian An and Art Owen. 2001. Quasi-regression. *Journal of complexity* 17, 4 (2001).
- [2] Vadim Arzamasov et al. 2018. Towards Concise Models of Grid Stability. In *2018 IEEE International Conference on Communications, Control, and Computing Technologies for Smart Grids (SmartGridComm)*.
- [3] Einat Neumann Ben-Ari and David M Steinberg. 2007. Modeling data from computer experiments: an empirical comparison of kriging with MARS and projection pursuit regression. *Quality Engineering* 19, 4 (2007).
- [4] Michael R Berthold and Klaus-Peter Huber. 1999. Constructing fuzzy graphs from examples. *Intelligent Data Analysis* 3, 1 (1999).
- [5] Leo Breiman. 1996. Bagging predictors. *Machine learning* 24, 2 (1996).
- [6] Leo Breiman. 2001. Random forests. *Machine learning* 45, 1 (2001).
- [7] Benjamin P Bryant and Robert J Lempert. 2010. Thinking inside the box: a participatory, computer-assisted approach to scenario discovery. *Technological Forecasting and Social Change* 77, 1 (2010).
- [8] Cristian Bucilua et al. 2006. Model compression. In *Proceedings of the 12th ACM SIGKDD international conference on Knowledge discovery and data mining*.
- [9] Mark Craven and Jude W Shavlik. 1996. Extracting tree-structured representations of trained networks. In *Advances in neural information processing systems*.
- [10] Siddhartha Dalal et al. 2013. Improving scenario discovery using orthogonal rotations. *Environmental modelling & software* 48 (2013).
- [11] Pedro Domingos. 1997. Knowledge Acquisition from Examples Via Multiple Models. In *Proceedings of the Fourteenth International Conference on Machine Learning* (1997).
- [12] Alexander Forrester et al. 2008. *Engineering design via surrogate modelling: a practical guide*.
- [13] Alex A Freitas. 2014. Comprehensive classification models: a position paper. *ACM SIGKDD explorations newsletter* 15, 1 (2014).
- [14] Jerome Friedman and Nicholas Fisher. 1999. Bump hunting in high-dimensional data. *Statistics and Computing* 9, 2 (1999).
- [15] Dirk Gorissen et al. 2010. A surrogate modeling and adaptive sampling toolbox for computer based design. *Journal of Machine Learning Research* 11, Jul (2010).
- [16] David G Groves and Robert J Lempert. 2007. A new analytic method for finding policy-relevant scenarios. *Global Environmental Change* 17, 1 (2007).
- [17] Céline Guivarch et al. 2016. The diversity of socio-economic pathways and CO2 emissions scenarios: Insights from the investigation of a scenarios database. *Environmental modelling & software* 80 (2016).
- [18] David Hadka et al. 2015. An open source framework for many-objective robust decision making. *Environmental Modelling & Software* 74 (2015).
- [19] John H Halton. 1964. Algorithm 247: Radical-inverse quasi-random point sequence. *Commun. ACM* 7, 12 (1964).
- [20] Trevor Hastie et al. 2009. The elements of statistical learning: data mining, inference, and prediction, Springer Series in Statistics.
- [21] Jonathan D Herman et al. 2015. How should robustness be defined for water systems planning under change? *Journal of Water Resources Planning and Management* 141, 10 (2015).
- [22] Johan Huysmans et al. 2006. Using rule extraction to improve the comprehensibility of predictive models. Available at SSRN 961358 (2006).
- [23] Johan Huysmans et al. 2011. An empirical evaluation of the comprehensibility of decision table, tree and rule based predictive models. *Decision Support Systems* 51, 1 (2011).
- [24] Tsutomu Ishigami and Toshimitsu Homma. 1990. An importance quantification technique in uncertainty analysis for computer models. In *[1990] Proceedings. First International Symposium on Uncertainty Modeling and Analysis*.
- [25] Tushith Islam and Erik Pruyt. 2016. Scenario generation using adaptive sampling: the case of resource scarcity. *Environmental modelling & software* 79 (2016).
- [26] Gareth James et al. 2013. *An introduction to statistical learning*. Vol. 112.
- [27] Jack PC Kleijnen. 2015. Design and analysis of simulation experiments. In *International Workshop on Simulation*.
- [28] JH Kwakkel and SC Cunningham. 2016. Improving scenario discovery by bagging random boxes. *Technological Forecasting and Social Change* 111 (2016).
- [29] Jan H Kwakkel and Marc Jaxa-Rozen. 2016. Improving scenario discovery for handling heterogeneous uncertainties and multinomial classified outcomes. *Environmental modelling & software* 79 (2016).
- [30] Jan H Kwakkel and Erik Pruyt. 2013. Exploratory Modeling and Analysis, an approach for model-based foresight under deep uncertainty. *Technological Forecasting and Social Change* 80, 3 (2013).
- [31] Robert J Lempert et al. 2006. A general, analytic method for generating robust strategies and narrative scenarios. *Management science* 52, 4 (2006).
- [32] Robert J Lempert et al. 2008. Comparing algorithms for scenario discovery. *RAND, Santa Monica, CA* (2008).
- [33] Crystal Linkletter et al. 2006. Variable selection for Gaussian process models in computer experiments. *Technometrics* 48, 4 (2006).
- [34] Jason L Loeppky et al. 2013. Global sensitivity analysis for mixture experiments. *Technometrics* 55, 1 (2013).
- [35] Hyejung Moon. 2010. *Design and analysis of computer experiments for screening input variables*. Ph.D. Dissertation. The Ohio State University.
- [36] Max D Morris et al. 2006. Sampling plans based on balanced incomplete block designs for evaluating the importance of computer model inputs. *Journal of Statistical Planning and Inference* 136, 9 (2006).
- [37] Jeremy E Oakley and Anthony O’Hagan. 2004. Probabilistic sensitivity analysis of complex models: a Bayesian approach. *Journal of the Royal Statistical Society: Series B (Statistical Methodology)* 66, 3 (2004).
- [38] Victor Picheny et al. 2013. A benchmark of kriging-based infill criteria for noisy optimization. *Structural and Multidisciplinary Optimization* 48, 3 (2013).
- [39] Henri Pierreval. 1992. Rule-based simulation metamodels. *European Journal of Operational Research* 61, 1-2 (1992).
- [40] Andrea Saltelli et al. 2000. *Sensitivity Analysis*.
- [41] Thomas J Santner et al. 2003. *The design and analysis of computer experiments*. Vol. 1.
- [42] Benjamin Schäfer et al. 2015. Decentral smart grid control. *New journal of physics* 17, 1 (2015).
- [43] Burr Settles. 2009. *Active learning literature survey*. Technical Report. University of Wisconsin-Madison Department of Computer Sciences.
- [44] Timothy W Simpson et al. 2001. Metamodels for computer-based engineering design: survey and recommendations. *Engineering with computers* 17, 2 (2001).
- [45] IM Sobol and Yu L Levitan. 1999. On the use of variance reducing multipliers in Monte Carlo computations of a global sensitivity index. *Computer Physics Communications* 117, 1 (1999).
- [46] S. Surjanovic and D. Bingham. [n. d.]. Virtual Library of Simulation Experiments: Test Functions and Datasets. <http://www.sfu.ca/~ssurjano>
- [47] Geoffrey G Towell and Jude W Shavlik. 1993. Extracting refined rules from knowledge-based neural networks. *Machine learning* 13, 1 (1993).
- [48] Evelina Trutnevte et al. 2016. Reinvigorating the scenario technique to expand uncertainty consideration. *Climatic change* 135, 3-4 (2016).
- [49] Laura Uusitalo et al. 2015. An overview of methods to evaluate uncertainty of deterministic models in decision support. *Environmental Modelling & Software* 63 (2015).
- [50] Michael Wainberg et al. 2016. Are random forests truly the best classifiers? *The Journal of Machine Learning Research* 17, 1 (2016).
- [51] Warren E Walker et al. 2013. *Deep Uncertainty*.
- [52] G Gary Wang and Songqing Shan. 2007. Review of metamodeling techniques in support of engineering design optimization. *Journal of Mechanical design* 129, 4 (2007).
- [53] William J Welch et al. 1992. Screening, predicting, and computer experiments. *Technometrics* 34, 1 (1992).
- [54] Brian Williams et al. 2006. Combining experimental data and computer simulations, with an application to flyer plate experiments. *Bayesian Analysis* 1, 4 (2006).
- [55] Taketoshi Yoshida and Shinichi Nakasuka. 1989. A dynamic scheduling for flexible manufacturing systems: hierarchical control and dispatching by heuristics. In *Proceedings of the 28th IEEE Conference on Decision and Control*.

A DESCRIPTIONS OF ALGORITHMS

In this section we provide the pseudo-code for the pasting step of PRIM and for the PRIM algorithm with bumping.

A.1 PRIM – Pasting Step

The pasting step of the PRIM (Algorithm 3) receives the data d , the initial box containing it – box_0 , the pasting parameter β and the box to be expanded – box . It repeatedly expands the box along any dimension so that the mean value of y of the points from d inside the resulting box increases (Lines 10, 14). Let the box be described with the inequalities $x_i^- \leq x_i \leq x_i^+$, $i = 1, \dots, D$. The operation $box_{new} = \text{expand}(box, z)$ changes the value z in the box description, so that the volume of box_{new} is greater than that of box by $1 + \beta$. The algorithm stops when no further expansion is possible (Line 2).

Algorithm 3: PRIM.paste (pasting step)

Data: d, β, box, box_0 – as described in the text

Result: expanded hyperbox.

```

1 boxes = box;
2 while boxes <> {} do
3   box = sample.one.box.randomly(boxes);
4   d_in = d : d.x ∈ box;
5   m = avg(d_in.y);
6   boxes = {};
7   for 1 ≤ i ≤ D do
8     box+ = expand(box, xi+);
9     d+ = d : d.x ∈ box+;
10    if avg(d+.y) > m & box \ box0 = ∅ then
11      boxes = append(boxes, box+);
12    box- = expand(box, xi-);
13    d- = d : d.x ∈ box-;
14    if avg(d-.y) > m & box \ box0 = ∅ then
15      boxes = append(boxes, box-);
16 return box

```

A.2 PRIM with Bumping

Algorithm 4 describes the PRIM algorithm with bumping. The notation used is the same as in Section 3.2.

B EXPERIMENT WITH MSE

In this section we describe how we conducted experiments with MSE in Section 5.2. We then present results of such experiments with another DGP, which provide additional insights.

Experimental setting. In our experiment we created independently 200 datasets d of size $N = 400$ labeled with the selected DGP. For each dataset d_i we trained one random forest model, f_i^a and let it label 100 datasets d_{new}^{ij} . Additionally, we created a large dataset d_{gt} of 10^6 points and labeled it with the selected DGP. For a fixed box b we calculate MSEs as follows.

$$MSE_O = \text{Var}(\hat{\mu}) = \sum_{i=1}^{200} (\hat{\mu}_i)^2 / 200 - \left(\sum_{i=1}^{200} \hat{\mu}_i / 200 \right)^2$$

Algorithm 4: PRIM with bumping

Data: $d, d_{val}, \alpha, box_0, minpts, t, T$ – as described in the text

Result: sequence of hyperboxes

```

1 boxes = {};
2 for 1 < i < T do
3   dbs = bootstrap sample from d;
4   S = {xr1, ..., xrt} – random subset of attributes;
5   dbsS = dbs with attributes in S;
6   dvalS = dval with attributes in S;
7   boxesi = PRIM.peel(d = dbsS, dval = dvalS, ...);
8   boxes = append(boxes, boxesi);
9 boxes = non.dominated(boxes);
10 return boxes

```

$$\text{Bias}(\hat{\mu}_i^a) = \mu_{gt} - \sum_{j=1}^{100} \hat{\mu}_{ij}^a / 100,$$

$$\text{Var}(\hat{\mu}_i^a) = \sum_{j=1}^{100} (\hat{\mu}_{ij}^a)^2 / 100 - \left(\sum_{j=1}^{100} \hat{\mu}_{ij}^a / 100 \right)^2$$

$$MSE_{AM} = \sum_{i=1}^{200} (\text{Bias}(\hat{\mu}_i^a) + \text{Var}(\hat{\mu}_i^a))$$

Here we use indexes i for enumerating datasets d_i and j for indexing datasets d_{new}^{ij} , and keep the other notations as in Section 5. We have also substituted μ in (6) with

$$\mu_{gt} = \sum_r y_{gt}^r \quad y_{gt}^r = f(d_{gt}.x^r) \quad r : d_{gt}.x^r \in b$$

Additional experiments. We conducted the experiments described above and in Section 5.2 with four DGPs: ‘3’, ‘8’, ‘linketal06simple’ and ‘morris’. In all experiments we calculated MSEs of the mean estimates of labels in $2 \cdot D$ boxes, considered as candidates for cutting off at the first iteration of PRIM. When the metamodel is random forest, which outputs class labels, we have obtained $MSE_O > MSE_{AM}$ (when $K = 10^5$) for majority of boxes for the first three DGPs. For DGP ‘morris’ for all $2 \cdot D = 40$ boxes the relation was opposite: $MSE_O < MSE_{AM}$. However, one sees (Table 9) that in this case our method is by far better than the original one.

Let us index these 40 boxes with r . The detailed analysis reveals that μ_{gt}^r for $r \in rset = \{8, 9, 10\}$ are significantly lower than for other values of r . The share of cases, when $\min_r \hat{\mu}_i^r$ is reached for some $r^* \notin rset$ is 26%. Whereas, the share of cases, when $\min_r \hat{\mu}_{ij}^{a,r}$ is reached for some $r^* \notin rset$ is only 0.3%. That is, despite greater MSE, our method makes less irrelevant cutoffs. This is because that for each f_i^a the bias does not change the ranking of boxes by the mean value of labels of points they contain. All this might indicate, that the mechanism we described in Section 5 is not the unique one responsible for better performance of our approach.

C DGPS FOR EXPERIMENTS

Table 7 lists all 33 DGPs used in our study. The columns contain the following information. D is the number of inputs. $I \leq D$ is the number of ‘influential’ inputs, i.e., those defining the output. The

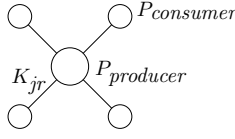


Figure 14: DSGC system structure

‘ref’ column contains the references to the work using respective function. A big share of functions we use are from [46]; we add the additional reference from this resource. As discussed before, we converted continuous function output to binary by specifying the threshold, so that $y = 1$ if the output is below it and $y = 0$ otherwise. The threshold values are in column ‘thr’. The functions, which already output $y \in \{0, 1\}$ have the values ‘na’ (not applicable) in this column. Finally, the expected share of outcomes $y = 1$ with uniform sampling of points from the input space is in column ‘share’.

In this paper we introduced the function ‘ellipse’ as follows:

$$y_e = \sum_{i=1}^{15} w_i \cdot (x_i - c_i)^2$$

where

$$\begin{aligned} w &\approx \{0.353, 0.434, 0.899, 0.373, 0.278, 0.164, 0.927, \\ &\quad 0.769, 0.975, 0.606, 0, 0, 0, 0\}, \\ c &\approx \{0.975, 0.843, 0.772, 0.325, 0.805, 0.945, 0.221, \\ &\quad 0.732, 0.289, 0.6, 0, 0, 0, 0\} \end{aligned}$$

D DECENTRAL SMART GRID CONTROL

Decentral smart grid control was proposed in [42] as novel approach realizing demand response without need in a centralized IT infrastructure. The key idea of it is to connect the electricity price to local frequency of electricity grid at each consumer or supplier. The dynamics of DSGC with N participants is described with the following N equations:

$$\begin{aligned} \frac{d^2\theta_j}{dt^2} &= P_j - \alpha_j \frac{d\theta_j}{dt} + \sum_{r=1}^M K_{jr} \sin(\theta_r - \theta_j) - \\ &\quad \frac{Y_j}{T_j} (\theta_j(t - \tau_j) - \theta_j(t - \tau_j - T_j)) \end{aligned} \quad (9)$$

The first (upper) part of equality is known as swing equation. It models the electrical grid as a system of connected rotating machines, each representing consumer or producer. Here θ_j is the phase of the j -th machine relative to the nominal grid frequency (e.g. 50 or 60 Hz); P_j is the nominal power demand/supply; α_j is damping constant – describes the tendency of the machine towards the nominal frequency; K_{jr} is coupling strength, characterizes the transmission line between j -th and r -th participants (equals 0 if there is no transmission line). The novelty of DSGC is in the last part of equation. It describes the process in which each participant measures the frequency ($d\theta_j/dt$) at its place, averages this frequency over the time period T_j and reacts by changing its electricity consumption or production with a time delay τ_j . The term Y_j is proportional to both coefficient connecting price to frequency and price elasticity of electricity demand or supply.

Table 7: AUC for different $|d|$

DGP	D	I	ref	thr	share (%)
1	5	2	[10]	na	47.6
2	5	2	[10]	na	25.7
3	5	2	[10]	na	8.2
4	5	2	[10]	na	18
5	5	2	[10]	na	8
6	5	2	[10]	na	8.1
7	5	2	[10]	na	35
8	5	2	[10]	na	10.9
102	15	9	[10]	na	67.2
borehole	8	8	[1, 46]	1000	30.9
dsgc	12	12	Sec D	na	53.7
ellipse	15	10	our	0.8	22.5
hart3	3	3	[46]	-1	33.5
hart4	4	4	[38, 46]	-0.5	30.1
hart6sc	6	6	[38, 46]	1	22.6
ishigami	3	3	[24, 46]	1	25.5
linketal06dec	10	8	[33, 46]	0.15	25.3
linketal06simple	10	4	[33, 46]	0.33	28.5
linketal06sin	10	2	[33, 46]	0	27.2
loepetal13	10	7	[34, 46]	9	38.9
moon10hd	20	20	[35, 46]	0	42.1
moon10hdc1	20	5	[35, 46]	0	34.2
moon10low	3	3	[35, 46]	1.5	45.6
morretal06	30	10	[36, 46]	-330	34.5
morris	20	20	[40]	20	30.1
oakoh04	15	15	[37, 46]	10	24.9
otlcircuit	6	6	[3, 46]	4.5	22.5
piston	7	7	[3, 46]	0.4	36.8
soblev99	20	19	[45, 46]	2000	41.3
sobol	8	8	[40]	0.7	39.2
welchetal92	20	18	[46, 53]	0	35.6
willetal06	3	2	[46, 54]	-1	24.9
wingweight	10	10	[12, 46]	250	37.8

Table 8: Input values used for DSGC simulations

Input	P	α	K	γ	τ	T
Consumers	-1	0.1	8	[0.05,1]	[0.5,5]	[1,4]
Producer	4			0	-	-

Simulations based of the equations described are used to ensure the stability of the DSGC for different combinations of inputs: P_j , α_j , K_{jr} , γ_j , T_j and τ_j . In the paper we simulate DSGC system of a particular structure presented on Figure 14. It is a ‘star’-like system, containing four consumers and one producer – in the center. We fixed the values of some inputs and sampled the others from a given ranges uniformly independently. See Table 8. In total there are 12 inputs that vary ($D = 12$): γ , T and τ for each electricity consumer.

E DETAILED EXPERIMENTAL RESULTS

Tables 9, 10, 11 and 12 contain the detailed results for AUC, density, interpretability and consistency respectively. For each DGP the

number of corresponding metric is averaged over 50 runs. For each dataset size $N = |d|$ and each DGP the number of best performing approach is in bold; for the second best approach the number is underlined. Rows 'avg', '# 1' and '# 2' are as explained in Section 8.

The columns 'D' and 'I' in Table 11 are the same as in Table 7. Finally, the last row in Table 12 is the average volume of the last box produced with each method, relative to the initial box size.

Table 9: AUC for different $|d|$

$ d $	400										800										1600									
	B	B.all	O	Op	RF.1	RF.p	B	B.all	O	Op	RF.1	RF.p	B	B.all	O	Op	RF.1	RF.p	B	B.all	O	Op	RF.1	RF.p						
1	43.3	42.6	41.9	41.9	43.8	44.3	44.1	43.9	43.8	43.8	44.2	44.5	44.5	44.4	44.4	44.4	44.4	44.4	44.5	44.4	44.4	44.4	44.4	44.8						
102	11.7	11	11	11	14.6	15.4	13.1	13.1	13	13.1	15.3	16	16	14.6	14.5	14.5	16.1	16.6	14.3	14.6	14.5	14.5	16.1	16.6						
2	67.3	66.8	67.2	67.1	67.7	68.1	68.1	67.9	67.8	67.8	67.7	68.3	68.3	68.7	68.5	68.4	68	68.7	68.7	68.5	68.4	68.4	68	68.7						
3	79	77.5	72.2	72.4	88.3	88.5	86.9	85.8	84.2	84.2	88.4	89.2	89.2	88.8	88.4	87.1	88.8	89.7	88.8	88.4	87.1	87.1	88.8	89.7						
4	63.6	60.7	60.5	60.4	67.7	68.7	67.6	66.8	66.2	66.1	68.7	69.4	69.4	69	68.5	68.3	69.2	69.6	69	68.5	68.3	68.3	69.2	69.6						
5	58.4	55	50.5	50.4	67.6	68.4	68.1	65.7	64.9	64.6	73.1	74.7	74.7	74.2	71.7	71.4	75.4	76.4	74.2	72.5	71.7	71.4	75.4	76.4						
6	75.7	76.3	69.7	69.8	86.5	86.3	86.6	85.9	83.9	83.9	88.4	88.8	88.8	88.7	88.4	87.2	89.2	89.4	88.7	88.4	87.2	87.2	89.2	89.4						
7	43.8	42	41.9	41.7	45.3	45.6	46.5	45.5	45.3	45.2	46.9	47.4	47.4	47.4	47.1	47	47.5	47.9	47.4	47.1	47.1	47	47.5	47.9						
8	63.5	61.7	60.1	60.3	71.9	73.3	71.4	69.8	69.6	69.5	74.5	75.9	75.9	75.6	74.6	73.8	75.7	77.2	75.6	74.6	73.8	73.6	75.7	77.2						
borehole	66.3	65.7	66.2	66.1	66.3	67.3	67.1	66.9	67	66.9	66.8	67.6	67.6	67.5	67.4	67.4	67.1	67.8	67.5	67.4	67.4	67.4	67.1	67.8						
dsgc	11	13.4	13.4	13.3	17	17.8	12.8	15.5	15.7	15.7	17.9	18.8	18.8	14.1	17.4	17.5	18.7	19.7	14.1	17.4	17.5	17.5	18.7	19.7						
ellipse	27.9	40.3	40.5	40.4	49	48.5	31	47.2	47.4	47.3	52.2	52.3	52.3	33.5	51.7	51.6	53.9	54.1	33.5	51.7	51.7	51.6	53.9	54.1						
hart3	58.2	57.5	57.1	56.8	59.1	59.5	59.6	59.2	59.2	59	60	60.4	60.4	60.2	60.1	60	60.4	60.7	60.2	60.1	60.1	60	60.4	60.7						
hart4	46.6	48.4	47.3	47.1	51.5	51.8	49.6	50.7	49.5	49.4	52.9	53.2	53.2	50.8	52.9	52.4	53.9	54.3	50.8	52.9	52.4	52.4	53.9	54.3						
hart6sc	26.3	33.2	30.2	30.2	42.6	42.3	29.9	40.2	37.8	37.9	44.8	45.3	45.3	33.1	43.7	43	45.8	46.3	33.1	43.7	43	42.9	45.8	46.3						
ishigami	23.3	23.1	20.2	20.2	22.8	22.7	24	24.4	22.5	22.7	23.1	23.4	23.4	23.9	24.3	22.8	23.3	23.4	23.9	24.3	22.8	22.8	23.3	23.4						
linketal06dec	56.9	54.3	53	53.1	61.6	62	60.7	59.1	58.7	58.7	62.5	63	63	62.6	61.7	61.2	63.1	63.5	62.6	61.7	61.2	61.2	63.1	63.5						
linketal06simple	34.7	36.2	35.8	35.9	43.8	43.7	40.2	42.3	42	42	44.6	45	45	42.8	45.8	45.8	46.9	47	42.8	45.8	45.8	45.8	46.9	47						
linketal06sin	67.7	65.9	65.9	65.8	68.8	69.7	69.1	68.5	68.4	68.3	69.4	70	70	69.9	69.7	69.8	69.9	70.4	69.9	69.7	69.8	69.7	69.9	70.4						
loepetal13	39.7	38.1	37.4	37.4	43.2	43.5	42.9	42.4	42.6	42.5	44.3	44.7	44.7	44.2	44.1	43.9	44.8	45	44.2	44.1	43.9	43.9	44.8	45						
moon10hd	14.2	13.3	12.6	12.5	23.1	23	17.6	17.4	17.3	17.3	24.9	24.8	24.8	20.1	20.6	21	25.3	25.3	20.1	20.6	21	21	25.3	25.3						
moon10hdcl1	24.5	18.7	18	18	36.5	36.9	31.7	26.8	27.3	27.3	37.3	37.9	37.9	35.3	33.1	33.4	37.6	38.3	35.3	33.1	33.4	33.4	37.6	38.3						
moon10low	43.1	42.3	42	42	44	44.3	43.9	43.8	43.5	43.5	44.4	44.7	44.7	44.5	44.3	44.2	44.7	44.9	44.5	44.3	44.2	44.1	44.7	44.9						
morretal06	13.7	14	13.9	13.9	22.2	22.3	17.3	18.5	18.8	18.7	24.1	23.9	23.9	19.7	22.3	23.1	24.8	24.7	19.7	22.3	23.1	23	24.8	24.7						
morris	12	10.4	9.2	9.2	25.2	25.2	16.9	15.1	14.3	14.4	27.5	27.1	27.1	21.8	20.9	21	28.7	28.5	21.8	20.9	21	21	28.7	28.5						
oakoh04	17.9	15.7	15.2	15.2	28.1	28	23.3	21.1	21.1	21.2	29.8	29.7	29.7	26.4	25.9	26	31.1	31	26.4	25.9	26	26.1	31.1	31						
otlcircuit	56.8	55.7	54.1	54	61.4	61.7	60.8	59.2	59.3	59.2	62.3	62.6	62.6	62.2	61.9	61.6	63.4	63.4	62.2	61.9	61.6	61.5	63.4	63.4						
piston	50.9	49.2	47.9	47.7	52.4	53	52.8	52	51.6	51.5	53.2	53.6	53.6	53.3	53.1	52.9	53.8	53.8	53.3	53.1	53.1	52.9	53.6	53.8						
sobley99	18.4	18.1	17.9	17.9	26.6	26.5	21.3	22.4	22.4	22.4	27.4	27.1	27.1	23.6	25.4	25.7	28.2	28.1	23.6	25.4	25.7	25.7	28.2	28.1						
sobol	53.1	51.2	51.1	51.1	53.8	54.3	54.6	53.9	53.8	53.8	54.6	55.1	55.1	55.4	55.1	55	55.2	55.6	55.4	55.1	55	55	55.2	55.6						
welchetal92	38.9	37.5	36.8	36.8	44.8	44.8	42.8	42.4	41.9	41.9	46.4	47.4	47.4	45.1	45.3	45.6	47.9	48.6	45.1	45.3	45.6	45.6	47.9	48.6						
willettal06	69.7	69.5	69.6	69.5	70.8	71.3	71.3	71.1	71.4	71.2	72	72.3	72.3	72	72	72.1	72.4	72.6	72	72	72.1	72	72.4	72.6						
wingweight	34.9	33	31.7	31.8	40.2	40.7	38.6	37.6	37.1	37.1	41	41.4	41.4	39.8	39.8	39.7	41.3	41.6	39.8	39.8	39.7	39.7	41.3	41.6						
avg	42.8	42.4	41.3	41.2	48.7	49.1	46.4	46.7	46.4	46.3	50	50.5	50.5	48.3	49.3	49.1	50.8	51.2	48.3	49.3	49.1	49	50.8	51.2						
# 1	1	0	0	0	8	24	0	1	0	0	5	27	27	0	1	0	5	27	0	1	0	0	5	27						
# 2	0	1	0	0	24	8	4	0	0	0	24	8	8	4	0	0	24	8	6	0	0	0	22	5						

Table 10: Density for different $|d|$

$ d $	400						800						1600					
	B	B.all	O	O.p	RF.l	RF.p	B	B.all	O	O.p	RF.l	RF.p	B	B.all	O	O.p	RF.l	RF.p
1	97.5	96.6	96.1	96	97.9	98.8	98.4	98	98.2	98	98.3	99	98.9	98.7	98.7	98.7	98.6	99.3
102	85.1	84.4	84.1	84.1	92.3	95.1	88.9	88	88.5	88.5	94.1	96.7	91.9	92	92.2	92.3	96	97.9
2	94.9	94.4	94.5	94.4	94.8	95.5	95.4	95.2	95	94.8	95.9	95.9	96.2	95.8	95.8	95.9	95.1	96.4
3	92.3	94.4	91.9	92	98.5	98.7	97.6	97.7	97	96.9	98.5	99.2	98.9	98.7	97.4	97.4	98.7	99.8
4	89.2	86.6	86.9	86.8	93.6	95.3	93.8	93.4	92.9	92.8	94.5	96	95.5	94.8	94.8	94.6	95.3	96.3
5	74.1	73.7	71	71	84.1	84.7	83.9	82.9	82	81.4	91.5	92.7	92.6	90.4	89.6	88.8	94.4	95.7
6	88.8	92.8	89.8	89.7	97.2	97.1	97.7	97.6	95.8	95.7	98.7	99	99	98.8	97.6	97.6	99.4	99.6
7	91.1	88.3	88.8	88.2	92.6	93.8	95.6	93.7	93.9	93.5	95.2	96.7	97.2	96.3	96.6	96.3	96.7	98
8	81.1	80.6	79.9	80.2	89.2	91	89.7	88.3	88.5	88.3	92.9	95.1	95.2	93.8	93	92.4	94.3	97.2
borehole	98.3	98	98	97.9	98.1	99.3	99	98.9	98.8	98.7	98.5	99.6	99.4	99.3	99.3	99.3	99	99.8
dsgc	71.1	77.1	77	76.7	87.7	90.7	74.4	82.7	83.8	83.7	91	95.3	77.3	88.8	88.7	88.7	93	97.8
ellipse	56.1	74.8	75.9	75.7	91.5	92.5	61.6	84.2	83.5	83.3	95.1	96.8	65.4	90.5	89.4	89.2	96.3	98
hart3	96.6	95.9	95.7	95.1	97.4	98	98.3	97.6	98	97.5	98.5	99.1	99	98.9	99.1	98.8	99.3	99.7
hart4	87.4	90.9	89.7	89	94	95.2	94.7	93.6	93.3	92.8	96.1	97.1	96.9	96.5	96.8	96.5	97.7	98.8
hart6sc	60.5	77.7	74.4	74.1	92.4	92.4	66.3	88	87.7	87.4	94.7	96.4	74.5	92.9	93.1	92.6	95.7	97.6
ishigami	55	54.6	50.8	50.8	52.7	52.5	58	59.8	53.7	54.4	53.1	53.8	60	62.1	54.2	54.2	53.3	53.5
linketal06dec	90.2	87.9	86.7	86.7	95.7	96.7	95	93	92.5	92.4	97.2	98.3	97.6	96.1	95.5	95.6	98	98.8
linketal06simple	75	79.1	79.6	79.7	94.2	95.4	86.6	87.9	87.5	87.5	96.2	97.3	92.8	93.5	93.6	93.6	98	98.6
linketal06sin	97	95.2	94.9	94.7	97.4	98.6	98.2	97.4	97.3	97.2	98.3	99.1	99.1	98.8	98.9	98.8	99	99.7
loepetal13	90.3	87.7	88.4	88	96.1	96.6	95.1	93.9	94.5	94.3	97.7	98.6	97.6	96.7	96.8	96.7	98.6	99.2
moon10hd	63.6	63	62.8	62.7	86.3	87	70.8	71.9	72.2	72.1	92.6	93.5	76	78.7	80.4	80.3	95.1	96.2
moon10hdc1	70	62.9	62.7	62.7	91.2	93.9	83.4	73.6	75.5	75.4	93.2	95.5	90.7	83.4	85.5	85.4	94.4	97
moon10low	96.8	95.9	96.3	96.2	97.6	98.2	97.8	97.8	98	97.9	98.4	98.9	99	98.7	98.9	98.8	99.2	99.5
morretal06	55.4	58.2	57.6	57.6	82.2	84.6	61.7	66.5	66.1	65.9	90	91.3	68.4	72.7	74.5	74.4	93.1	95.2
morris	47.1	48.3	47.2	47.2	79.4	81.5	57.6	55.2	56.2	56.1	86	88.1	70.3	67.9	69.3	69.2	87.5	92.4
oakoh04	53.3	52.4	52.9	52.9	79.1	80.4	64.6	61.8	63.7	63.9	87.3	89.6	73.1	74.5	74.3	74.4	92	94.5
otlcircuit	88.2	88.8	87.3	87.1	95.3	95.9	94.9	92.6	93.2	92.9	96.8	97.7	96.7	96.1	96.1	95.8	97.7	98.6
piston	95.4	93.8	93.2	92.7	97.5	98.5	98	96.7	96.6	96.4	98.4	99.2	98.8	98.4	98.4	98.2	99.2	99.6
soblev99	70	70	69.8	69.7	92.1	92.7	76.4	77	78	78	96.2	95.9	82.9	83.5	85	84.8	98	97.9
sobol	96.7	94.6	94.6	94.4	97.3	98.4	98.4	97.5	97.5	97.4	98.1	99	99.3	98.9	98.8	98.8	98.8	99.6
welchetal92	80	78.3	78	77.9	87.4	90.8	86.1	84.5	84	83.9	90.3	94.6	89.6	88.5	89.8	89.8	93.4	97
willetal06	96.4	96.3	96.4	96.2	97.3	98	98.1	97.9	98.2	97.9	98.8	99.2	99	99	99	98.9	99.4	99.7
wingweight	85.3	83.7	83	83.1	95.8	96.9	92	90.4	90.3	90.2	97.4	98.2	95	94.3	94.3	94.1	98.6	99
avg	80.9	81.7	81.1	80.9	91.4	92.6	86.3	87.1	87	86.9	93.9	95.2	89.8	91.2	91.1	90.9	95.2	96.6
#1	1	0	0	0	2	30	0	1	0	0	1	31	0	1	0	0	1	31
#2	2	1	0	0	28	2	6	0	0	0	26	1	10	0	0	0	22	1

Table 11: Number of restricted dimensions for different $|d|$

method	400					800					1600										
	B	Ball	O	Op	RF.p	B	Ball	O	Op	RF.p	B	Ball	O	Op	RF.p	B	Ball	O	Op	RF.p	D
1	2.68	3.76	3.98	3.96	2.14	3.04	2.5	3.18	3.56	3.5	2.1	3.12	2.72	3.44	3.76	3.86	2.22	3.82	5	2	
102	3.98	13	12.5	12.5	7.28	9.4	3.98	13.4	12.7	12.7	6.6	9.34	3.98	13.4	12.6	12.6	6.78	9.3	15	9	
2	<u>2.62</u>	3.46	3.6	3.68	1.74	3.58	<u>2.82</u>	4.22	4.26	4.34	2.12	4.24	<u>2.94</u>	4.74	4.72	4.74	2.02	4.64	5	2	
3	2.76	4.2	3.8	3.74	2.02	2.02	2.34	2.66	2.6	2.58	2.02	<u>2.12</u>	<u>2.06</u>	2.08	2.08	2.08	2	2.18	5	2	
4	2.9	4.5	4.44	4.46	2.36	3.2	<u>2.92</u>	4.6	4.46	4.54	2.46	3.68	<u>3</u>	4.56	4.34	4.44	2.5	4.38	5	2	
5	<u>2.88</u>	4.62	4.7	4.7	2.28	2.3	<u>2.82</u>	4.48	4.48	4.52	2.42	2.8	<u>2.9</u>	4.3	4.42	4.46	2.32	3	5	2	
6	2.86	4.32	4.04	4.04	2.02	2.02	2.24	2.74	2.42	2.42	2.52	<u>2.06</u>	<u>2.08</u>	2.1	2.1	2.1	2	2.28	5	2	
7	2.96	4.54	4.4	4.4	2.68	3.64	2.9	4.4	4.16	4.18	2.52	3.4	<u>2.7</u>	3.96	3.82	3.82	2.26	3.7	5	2	
8	2.94	4.52	4.46	4.48	2.48	<u>2.74</u>	<u>2.88</u>	4.48	4.48	4.52	2.58	2.94	<u>2.9</u>	4.4	4.24	4.28	2.6	3.62	5	2	
borehole	<u>1.36</u>	1.8	1.7	1.68	1.06	1.68	<u>1.3</u>	1.4	1.72	1.72	1.06	1.76	<u>1.16</u>	1.36	1.52	1.5	1.04	1.94	8	8	
dsgc	3.98	11.2	11.4	11.4	9.74	10.7	<u>4</u>	11.8	11.5	11.5	10.3	11.5	<u>4</u>	11.9	11.7	11.7	10.2	11.7	12	12	
ellipse	<u>4</u>	12.3	11.7	11.7	<u>6.46</u>	6.9	3.98	12.6	11.1	11.1	<u>7.16</u>	7.94	<u>4</u>	12.4	10.9	10.9	<u>7.34</u>	8.76	15	10	
hart3	2	2.52	2.66	2.6	2.28	2.38	2	2.46	2.44	2.42	2.08	2.3	2	2.4	2.28	2.28	2.2	2.48	3	3	
hart4	2	3.92	3.94	3.94	<u>3.52</u>	3.8	2	3.92	3.92	3.92	<u>3.78</u>	3.94	2	3.94	3.94	3.94	<u>3.8</u>	4	4	4	
hart6sc	3	5.88	5.92	5.92	<u>5.3</u>	5.38	3	5.96	5.92	5.9	<u>5.4</u>	5.64	3	5.9	5.94	5.94	<u>5.44</u>	5.68	6	6	
ishigami	1.86	2.48	2.02	2.12	1	1	1.88	2.64	1.7	1.88	1	1	1.96	2.48	2.2	2.32	1	1	3	3	
linketal06dec	3.7	7.64	7.38	7.5	2.52	3.36	3.74	7.32	7.04	6.98	2.58	3.4	3.6	5.88	6.28	6.2	2.46	3.66	10	8	
linketal06simple	3.86	8.9	8.92	8.88	3.92	3.98	3.98	8.9	8.6	8.54	3.9	4.1	3.98	8.04	7.76	7.74	4.02	4.06	10	4	
linketal06sin	2.56	4.36	4.36	4.3	1.46	1.88	<u>1.94</u>	2.9	3.3	3.28	1.38	1.96	<u>1.76</u>	2.22	2.24	2.24	1.28	1.82	10	2	
loepetal13	3.84	7.84	8	8.12	2.76	3.22	3.94	7.6	6.78	6.78	2.76	<u>3.2</u>	3.76	6.16	6.24	6.12	2.96	3.28	10	7	
moon10hd	4.98	15.9	16.4	16.4	<u>7.14</u>	7.32	4.98	16.7	16.3	16.3	<u>8.92</u>	9.6	<u>5</u>	18	16.4	16.4	<u>10.2</u>	10.3	20	20	
moon10hdc1	<u>4.72</u>	15	15.9	15.9	3.4	4.74	4.9	15.8	14	14	3.9	5.42	<u>4.84</u>	16.3	13.6	13.6	3.56	6.44	20	5	
moon10low	1.98	2.84	2.92	2.92	2.04	2.28	1.94	2.76	2.86	2.86	2	2.42	<u>1.96</u>	2.7	2.82	2.82	2.08	2.64	3	3	
morretal06	5.88	20.1	20.5	20.6	6.74	7.32	5.92	21.7	20.4	20.3	8.34	8.68	6	23.3	20.7	20.8	<u>9.42</u>	9.48	30	10	
morris	4.94	16.7	17.1	17.1	4.58	4.94	4.98	17.4	17.3	17.3	<u>6.2</u>	7.74	4.98	17.3	16.8	16.9	<u>6.82</u>	10.6	20	20	
oakoh04	3.92	13.3	13.4	13.4	3.92	4.22	3.96	13.7	13.4	13.4	<u>5</u>	5.52	3.98	13.5	13.4	13.4	<u>5.94</u>	6.42	15	15	
otlrcircuit	3	5.42	5.42	5.44	<u>3.12</u>	3.54	3	5.4	5.34	5.38	<u>3.34</u>	3.68	<u>3</u>	5.24	5.04	5.04	<u>3.34</u>	3.94	6	6	
piston	2.88	5.46	5.54	5.48	2.04	2.16	2.68	3.88	4.3	4.3	2.12	2.2	2.48	3	3.4	3.36	<u>2</u>	2.42	7	7	
soblev99	4.88	16	15.6	15.6	6.76	7.3	4.98	16.8	15.5	15.5	<u>7.42</u>	7.74	4.96	16.8	15.5	15.5	8.1	7.94	20	19	
sobol	2.2	4.2	3.84	3.84	2.08	3.36	1.8	2.9	2.98	2.98	1.68	3.04	<u>1.52</u>	2.38	2.52	2.52	1.46	2.84	8	8	
welchetal92	4.8	13.2	12.4	12.4	<u>7.14</u>	9.9	4.9	15.1	12.9	12.9	<u>6.54</u>	10.5	4.96	15	12.4	12.4	<u>5.8</u>	10.7	20	18	
willetal06	1.98	2.38	2.44	2.42	1.98	2	<u>2</u>	2.06	2.26	2.26	<u>2</u>	2.02	2	2.02	2.12	2.12	<u>2</u>	2.02	3	2	
wingweight	<u>3.98</u>	8.68	8.88	8.88	3.8	4.68	<u>3.98</u>	9.04	8.32	8.38	3.94	5.04	3.98	8.48	7.9	7.94	<u>4.4</u>	5.12	10	10	
avg	3.3	7.72	7.71	7.71	3.63	4.24	3.25	7.72	7.36	7.37	3.87	4.67	3.22	7.57	7.14	7.14	3.99	5.04			
#1	15	0	0	0	20	3	15	0	0	0	19	1	17	0	0	0	17	1			
#2	9	0	0	0	13	7	11	0	0	0	14	6	13	0	0	0	15	3			

Table 12: Consistency for different $|d|$

d	400						800						1600					
	B	Ball	O	Op	RF1	RFp	B	Ball	O	Op	RF1	RFp	B	Ball	O	Op	RF1	RFp
1	60.9	61.7	53.7	55.6	74.9	62.4	62.6	67.9	58	60.6	76.7	63.2	57.2	60.6	56.9	56.3	77.7	56.5
102	12.4	22.1	26.4	26.7	22.3	23.9	9	19.3	22.4	22.8	23.5	25.1	6.7	18.5	22.1	22.2	30.3	30.7
2	63	63	63.2	63.1	82.8	48.6	45.7	48	48.1	46.7	81.5	37.1	32.5	35.5	34.5	34.8	84.4	30.4
3	75.3	69.8	70	71.9	95	94.8	90.1	89.7	87.7	88.8	95.5	91.5	96.3	96.6	93.8	94.4	96.7	92.2
4	53.9	45.8	47.5	47.7	64.5	54.1	50.3	45.7	48.4	48.4	69.3	48.8	37.5	41	41.2	38.3	69.7	37.1
5	52.3	45	46.1	46.1	61.5	61.3	51.6	45.2	44.1	44.2	56.8	53.7	49.3	43.2	46.8	46.6	57.8	55.8
6	68.2	66.5	65.2	65.3	87.8	87.1	89.4	86.5	86.3	86.5	91.2	88.4	91.8	94	89.9	90	92.5	85.8
7	44.1	40.8	40.8	41.6	45.8	43.2	47.6	42.9	42.2	42.7	54.3	50.2	50.5	45.6	47.6	48.2	55.9	46.8
8	55	51.3	52.3	52.6	58.8	57.3	50	48.1	46.9	47.1	60.3	54.2	54.3	49.2	44.8	45.4	63.7	53.3
borehole	92.6	90.1	91.3	91.8	95.3	88.2	91	93.3	90.8	91.3	95.5	89.1	94.6	93.3	91.9	93	96.4	88
dsgc	10.5	19.4	23.5	23.7	23.8	26.4	7.1	17.8	21.8	22.3	28.3	32.2	4.9	20.7	25.9	25.3	33.2	41
ellipse	15.2	22.3	30.9	31.3	37.2	37.2	10.9	24	33.2	33.6	47	46.6	7.5	27.2	35.2	35.5	52.4	48.8
hart3	80.4	78.8	72.2	74.1	81.2	80.5	82.1	79.8	79.3	80.6	83.4	81.6	83.2	84.1	82.9	83.4	86.4	83.1
hart4	51.5	46.3	42.5	43	53.4	52.5	55.5	52.8	43.2	43.2	61.6	59.1	59.2	55.1	54.8	56.3	66.1	64
hart6sc	25	29.8	29.5	29.8	46.1	45.1	19.4	35.3	38.5	40	53.7	48.2	19.4	45.9	49.1	50.1	61.1	57.7
ishigami	21.5	24.9	27	25.5	32.1	28.3	12.9	14.2	18.9	19	17.8	20.6	10.2	11.5	9.1	9.6	14.6	14.6
linketal06dec	48.8	36.8	41.9	43.1	64.8	59.9	41.5	40.9	46.9	47.6	67	67	49	50.4	48.2	50.3	70.6	68.5
linketal06simple	21.8	24.7	28.2	29	36.6	41.3	21.1	29	32.2	33.8	35.2	43	19.5	34.7	39.4	39.6	41.9	49.9
linketal06sin	71.6	65.6	66.7	67.4	86.3	84.8	81.9	74	74	75	87.3	85.6	80.5	83.3	82.6	82.9	91.7	90.6
loepetal13	36.5	33.1	34.9	35	55.3	56.8	29.1	40	42.9	43.5	60.1	64	34.9	46.9	46	47.5	62	64.4
moon10hd	9.9	15.1	17.6	17.7	19.8	21	8.1	12.7	17.8	17.9	22.1	24.9	5.5	12.8	17.3	17.4	24.8	28
moon10hdci	16.6	15.3	19.6	19.7	33.9	30.1	15.8	14.2	21.2	21.4	35.9	30.7	15.5	15.4	21.2	21.5	33.8	28.3
moon10low	65.5	61.8	59.2	64.7	68.1	68.9	68	74	61.9	62.9	73	73.4	76.5	70	66.9	67.3	71.7	74.3
morretal06	7.4	13.1	17.9	17.9	9.4	9.9	5.9	10.6	16.3	16.4	10.3	12	3.5	9.9	15.2	15.2	10	13.2
morris	10.9	12.7	14.6	14.7	28.8	31.1	8.7	11.1	14.1	14.1	32.7	28.7	9.9	11.1	14.9	15.1	40.5	28.6
oakoh04	11.9	12.6	16.1	16.2	19.1	19.6	11.2	11.4	15.5	15.4	18.5	21.7	8	11	15.4	15.6	22.8	29.6
otlcircuit	48.4	43.1	40.6	41.1	54.3	57	46.3	41.5	45	44.6	54.1	57.5	39.9	49.8	49.4	50.4	56.4	58.7
piston	51.2	49.2	46.1	47.5	63.6	69.6	59.9	63.4	57.9	59.2	70	74.2	68.7	68.8	67.7	67.9	77.1	79.9
soblev99	11.9	16.4	19.9	20.2	18.4	20.8	7.8	14.5	19.9	20.1	20.5	25.6	5.7	15.4	19.7	20.1	23.2	31.5
sobol	71.4	61.6	64.3	64.5	77.7	65.2	79.6	71.9	70.7	70.9	81.5	70.2	86.2	80.4	77.6	77.7	88.9	76.5
welchetal92	25.4	25.9	32.2	32.7	40.7	29.7	19.3	22.1	29.6	30.2	43.4	30.1	14.2	20	29.7	30.1	45.2	32.3
willetal06	80.3	79.8	75.4	79	79.6	80.1	83.2	84.2	80.1	81	82.3	85	85.7	86.3	84.2	84.4	84.7	85
wingweight	26	24.6	29.2	29.4	41.1	45.4	23.5	28.7	31.2	30.9	44	48.2	19.1	32.7	36.2	36.8	45.6	50.7
avg	42.3	41.5	42.6	43.3	53.3	51	42	44.1	45.1	45.5	55.6	52.5	41.7	46.1	47.2	47.6	58.5	53.8
# 1	1	0	0	2	19	11	0	1	0	1	19	12	1	2	0	1	19	10
# 2	3	0	3	2	10	15	4	3	2	2	10	12	5	4	2	0	11	11
avg box vol.	14.3	13.4	13.9	14.3	12.9	11.4	11.1	11.3	11.9	12.2	11.7	9.9	9	9.9	10.4	10.6	10.9	8.7